INFLUENCE OF LASER POWER ON MORPHOLOGY AND PROPERTIES OF LASER-SINTERED UHMWPE

Y. Khalil[1], N. Hopkinson[2], A. Kowalski[3], J. P. A. Fairclough[1]

[1] Department of Mechanical Engineering, University of Sheffield, Sheffield S3 7HQ, UK
[2] XAAR plc, Cambridge Science Park, Cambridge, CB4 0XR, UK
[3] Unilever plc, R&D Port Sunlight Laboratory, Wirral CH63 3JW, UK

Abstract

Porous structures have unique physical properties (mechanical, density, etc.) that are related to their low density and architecture. These properties open a wide range of potential applications, such as biomedical, packaging, thermal insulation, filtering, food and beverage, pharmaceuticals, automobile, military and aerospace industries [1]. Laser Sintering is an additive manufacturing method that offers many advantages over conventional manufacturing techniques of porous structures with well-defined architectures, controllable pore sizes, excellent reproducibility, higher pore interconnectivities and improved mechanical properties can be produced accurately and rapidly.

This study describes the morphological and mechanical characterisations of porous Ultra-High Molecular Weight Polyethylene (UHMWPE) laser sintered parts to gain an insight into the correlation of process parameters and the morphological properties of these parts. Laser power was investigated to control the mechanical properties and porosity of the structures.

The fabricated parts were characterised through porosity measurements, three point flexural test and scanning electron microscopy (SEM). X-ray micro-computed tomography (micro-CT) was considered to evaluate the mean internal porosity as well as the size and spatial distribution of pores inside the structure of the UHMWPE parts aiming at a better understanding of the three-dimensional internal morphology of UHMWPE laser-sintered parts. The porosity was then compared with the porosity measured using the helium gas pycnometer method.

The results showed a high level of porosity in the UHMWPE laser-sintered parts with a range of 60-65% measured by micro-CT technique and helium gas pycnometer method respectively. There are no significant differences in the results obtained from both techniques and both results fit very well with each other. The results show that flexural strength decreases with an increase in porosity of the sintered parts.

Keywords Additive manufacturing, UHMWPE, Laser Sintering, Laser power, Micro computed tomography, Micro-CT

1. Introduction

Additive manufacturing (AM) offers remarkable opportunities for producing parts with complex internal structures that are impossible to produce with other manufacturing methods. Therefore, many AM parts have internal geometries that allow optimising the weight, shape and strength of these parts [2]. Laser Sintering (LS) is one of the AM techniques that has the capability to create a controlled complex geometry, both internally and externally, with a good dimensional accuracy and mechanical properties [3], [4]. However, LS parts can be prone to internal porosity. The mechanical properties of porous structures depend not only on the composition and the microstructure of the raw material, but also on the geometrical and morphological properties of the basic pore architecture [5].

Ultra High Molecular Weight Polyethylene (UHMWPE) is a thermoplastic polymer which is widely used in medical, industrial and consumer applications [6]. However, UHMWPE cannot be processed easily by injection moulding or melt extrusion due to its very high melt viscosity [7]. UHMWPE can be conventionally processed by compression moulding or ram extrusion [8] resulting in products with a density of 0.939 g/cm^3, flexural strength of 14.4 MPa and flexural modulus of 713 MPa [9].

Attempts have been made to produce UHMWPE parts using laser sintering with limited success. Rimell and Marquis attempted to laser sinter UHMWPE (GUR 4120 and GUR 4170) using a non-commercial LS machine. The study concluded that multiple layers cannot be produced due to material shrinkage, curling and degradation [10]. Goodridge et al attempted to laser sinter UHMWPE (GUR 4170) using the commercial Vanguard Laser Sintering machine (3D Systems). The mechanical properties of the laser sintered parts were investigated using tensile test and three point bend test. The average Ultimate Tensile Strength and Young's modulus reported were just above 0.2 MPa and 1.5 GPa respectively and the produced parts have an average flexural strength of 0.52 MPa with a modulus of 18.67 MPa. However, a limited success has been achieved as the sintered parts were only produced by using a precise combination of processing conditions [4].

To the authors' knowledge, no investigation has been reported related to the effect of process parameters on the porosity of UHMWPE laser sintered parts. This study describes the morphological and mechanical characterisations of porous UHMWPE laser sintered parts, built under different conditions, to gain an insight into the correlation of process parameters and the morphology properties of these parts. The laser power was investigated to control the mechanical properties and porosity of the structures. The difference in the porosity levels and the pores morphology between different LS parts were reported. The relationships between laser power, porosity and mechanical properties were discussed.

Micro-computed tomography (micro-CT) technique is a promising quality control method in AM that is able to perform non-destructive dimensional measurement of internal structures and non-destructive porosity measurement, which are serious issues in AM [2]. Previous studies investigated the pore size and the porosity distribution using micro-CT. Dupin et al [11] used micro-CT in their work and reported that the laser power has a significant impact on the porosity of polyamide 12 sintered parts. Rouholamin and Hopkinson [12] stated that micro-CT analysis can

be used as a non-destructive technique to assess the morphology of nylon 12 and measure the porosity and pore size of the laser sintered parts.

In this study, x-ray micro-CT was used to evaluate the porosity as well as the size and spatial distribution of pores inside the structure. This research establishes relationships between manufacturing process parameters (i.e. laser power), porosity and with mechanical properties (i.e. flexural properties).

2. Materials characterisation and parts manufacturing

2.1. Ultra-High Molecular Weight Polyethylene

The UHMWPE used in this study was supplied from Ticona/Celanese (Germany) as a powder, type GUR 2122, with a reported average particle size of 130 ±20 μm and molecular weight of 4.5×10^6 g/mol with a bulk density of the powder of 0.20 – 0.25 g/cm^3 (Celanese GUR® 2122 UHMWPE datasheet). However, the average particle size was determined to be 125 μm (d50), with a size distribution ranges from 46.2 μm (d10) to 293 μm (d90), as measured by laser light scattering using a Mastersizer 3000 (Malvern Instruments, UK) and the dry sample dispersion technique.

The peak temperature of the melting and recrystallisation of the UHMWPE powder was determined by Differential Scanning Calorimetry (DSC) (PerkinElmer Pyris DSC 8500) at a heating rate of 10°C/min. The peak temperatures of the melt and recrystallisation were 141 °C and 117 °C respectively.

Scanning electron microscopy (Philips XL-20, Holland, at 15 kV) was used to observe the UHMWPE powder microstructure. The images in Figure 1 show that the particles are non-spherical in shape with a highly agglomerated structure of smaller particles showing a cauliflower like appearance.
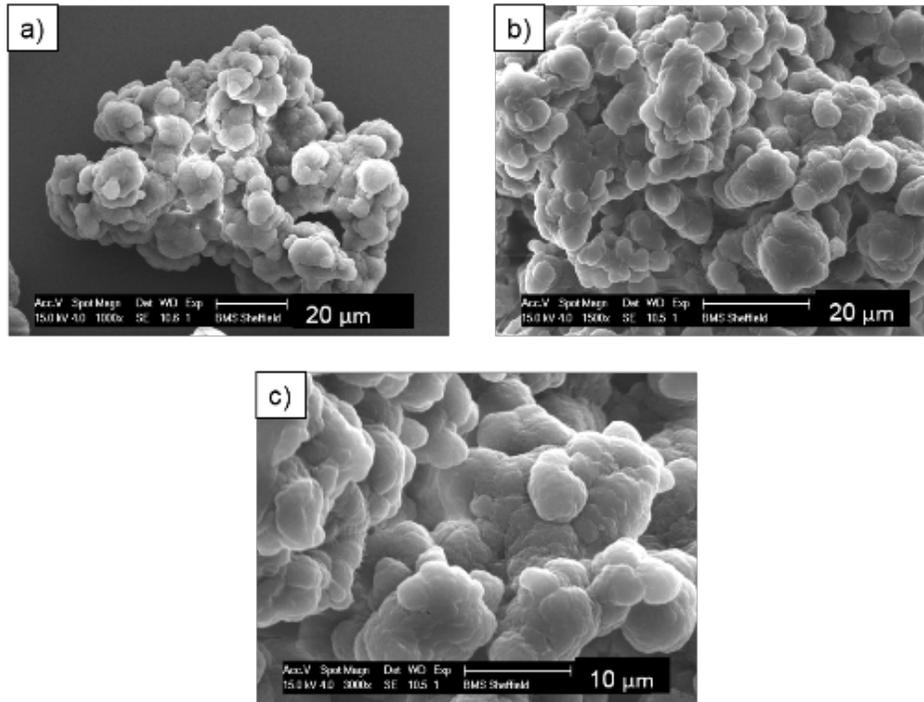
Figure 1: SEM micrographs of un-sintered UHMWPE powder
with magnifications: a) 1000x, b) 1500x and c) 3000x.

2.2. Part manufacture

Rectangular parts, 80 mm long, 10 mm wide and 4 mm thick, were fabricated using a commercial laser sintering system (EOS P100, Germany). The test parts were oriented in the x-y direction with the long axis parallel to the x-axis (Figure 2).
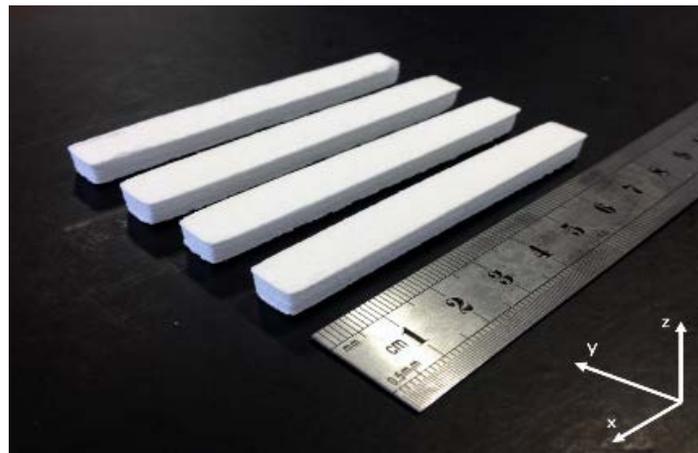

Figure 2: Laser sintered parts of UHMWPE

Four sets of test samples, four samples in each set, were fabricated at different laser powers of 6, 8, 10 and 12 watts. The laser scan speed, hatch spacing, powder bed temperature, removal chamber temperature and layer thickness were kept constant at 2500 mm/s, 0.15 mm, 142ºC, 135ºC and 0.1 mm respectively, with a double scan count.

3. Experimental procedures

This paper evaluates the successful test parts produced with various laser powers and characterises the porosity, mechanical properties, and microstructure of the sintered parts.

3.1. Porosity measurements

Small rectangular specimens with approximately 10 mm length, 8 mm width and 6 mm thickness, were cut out, from the centre and the end, of the laser sintered rectangular parts as shown in Figure 3. Three samples (A, B, and C) were used for density measurements and two samples (A and C) for morphology investigation. In this study, two methods were used to evaluate the porosity; micro computed tomography (micro-CT) and helium gas pycnometer.
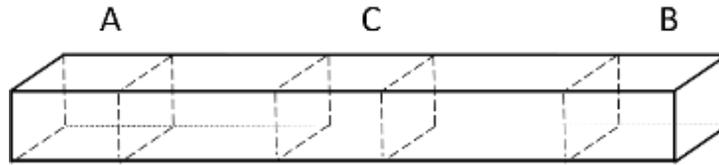

Figure 3: Density and morphology samples cut out from the laser sintered parts:
Samples A and B from the end and C from the centre

3.1.1. Helium gas pycnometer

To determine the part's porosity, the true density of the UHMWPE powder (ρ_{True}), the bulk density (ρ_{Bulk}) and skeletal density ($\rho_{Skeletal}$) of the sintered parts must be known. The bulk density of laser sintered parts was determined using a volumetric method as follows:

$$\rho_{Bulk} = \frac{m}{v} \qquad (1)$$

The mass of the parts was determined by weighing the samples using a digital balance and the volume of the parts was determined using Vernier callipers. The true density (or real density) of the UHMWPE powder and the skeletal density of the sintered parts were determined using Helium Gas Pycnometer (Micromeritics AccuPyc II 1340, USA). The true density of the UHMWPE powder was determined to be 0.954 g/cm³. The total, open and closed porosities were calculated using the following equatio

$$\text{Total porosity} = 1 - \left(\frac{\rho_{Bulk}}{\rho_{True}}\right) \times 100 \qquad (2)$$

$$\text{Open porosity} = 1 - \left(\frac{\rho_{Bulk}}{\rho_{Skeletal}}\right) \times 100 \qquad (3)$$

$$\text{Closed porosity} = \text{Total porosity} - \text{Open porosity} \qquad (4)$$

3.1.2. Micro-CT

The micro-CT technique is described by Ho and Hutmacher [13]. The internal microstructure of the laser sintered UHMWPE parts was investigated using Skyscan 1172 (Brucker μCT, Kontich, Belgium). The scanning conditions used were a current of 165 μA, voltage of 40 kV, pixel size of 5.9 μm, 360° rotation and 0.35° rotation step. SkyScan NRecon software (Bruker micro-CT, Kontich, Belgium) was used to reconstruct cross-section images from tomography projection images obtained from the scanner. CTAn software (Bruker micro-CT, Kontich, Belgium) was used for 3D morphological analysis of the micro-CT data (Figure 4).
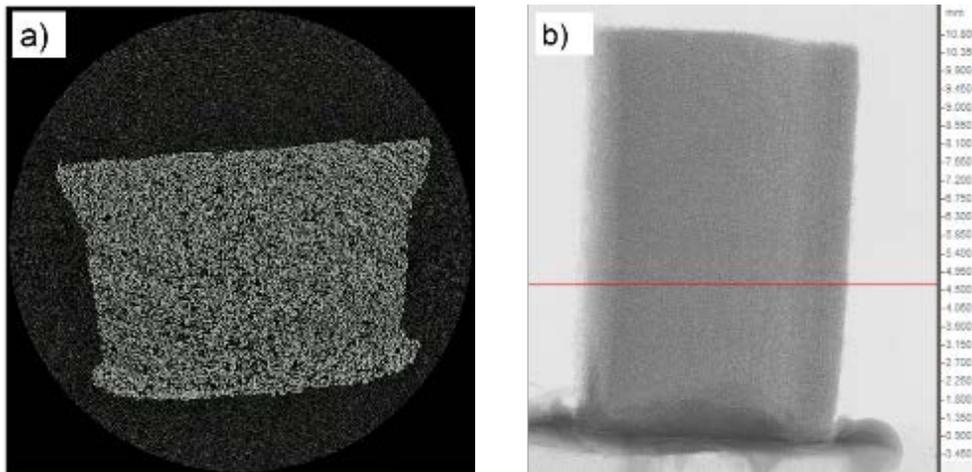

Figure 4: micro-CT images of LS part at 6 watts: a) Single 2D cross-section image (Pores in black colour), b) Reconstructed images to form 3D part. Red line indicates the position of the 2D image.

A cylindrical region of interest (ROI) with a diameter of 5 mm and a height of 8 mm was chosen for the 3D porosity analysis for all samples (Figure 5). CTVox software was used to show 3D representations of the structure.
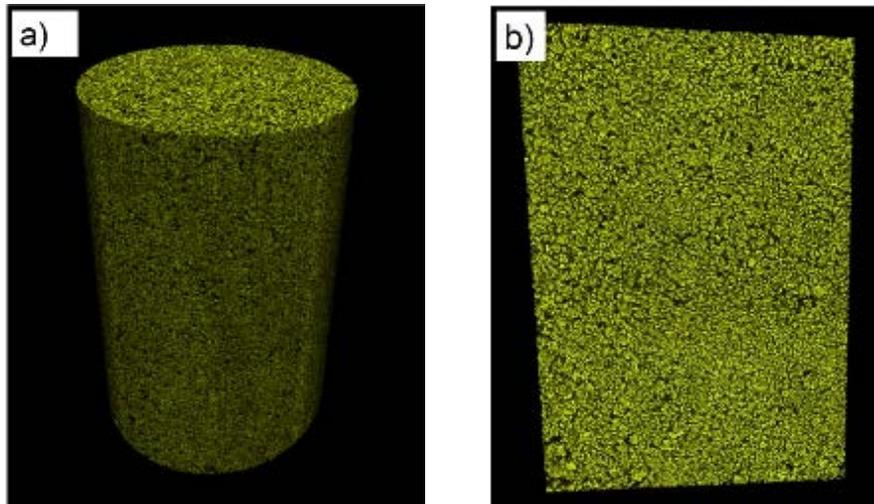
Figure 5: 3D representation of the part structure produced by CTVox
a) ROI created by CTAn b) Cross-section of the cylindrical ROI
(Pores in black colour)

3.2. Mechanical properties

Flexural properties were measured using three-point bending test on Texture Analyser TA500 machine (TM Lloyd Instruments, UK) fitted with a 500 N load cell. The support span length was 40 mm with a constant cross head speed of 2 mm/min. The results of the flexural tests were obtained by averaging the values over three test samples. All tests were performed at ambient temperature.

3.3. Scanning electron microscopy (SEM)

The external microstructure of the sintered parts was observed using a scanning electron microscope (Philips XL-20, Holland) at an accelerating voltage of 15 kV. All samples were gold sputtered before the observation to avoid charging.

4. Results and discussion

4.1. Morphological properties

Micro-CT technique was used on the UHMWPE porosity samples. Figures 6 and 7 show an image of a whole scanned sample and 2D images of cross-section respectively produced using CTAn software with regions of different densities in different colours. These images show that the density is varied from region to region in the 3D structure. Higher density areas are presented in a white and areas with low density including the pores are presented in black colour.
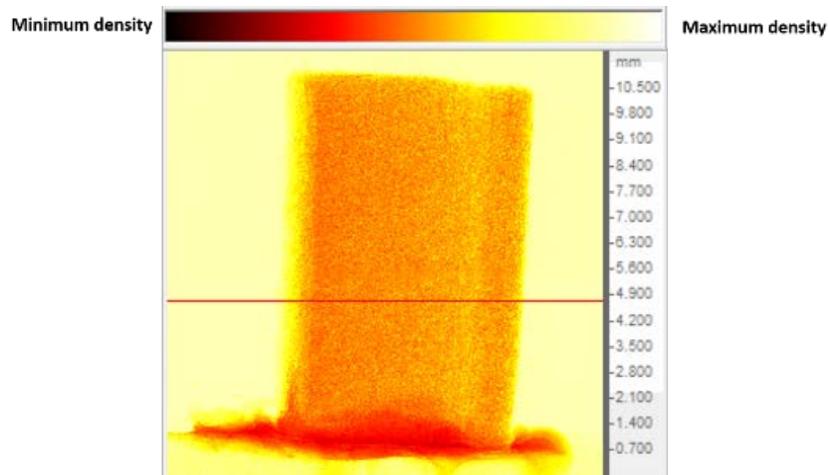
Figure 6: Reconstructed image of laser sintered sample
produced by CTAn software

As it can be seen in Figure 6, the results indicate a different density on the inside and in the outer area of the sintered part. The outer shell is more dense (yellow colour) than the inside of the part which is mainly in red to orange colour. Rüsenberg [14] indicated that the dense shell surrounding the part can be formed and strongly influenced by the thickness of the sample and the cooling rate. Ajuku [15] also reported the same phenomenon and suggested that the short bursts of energy at the edges result in parts being much denser at the edges than at the centres.
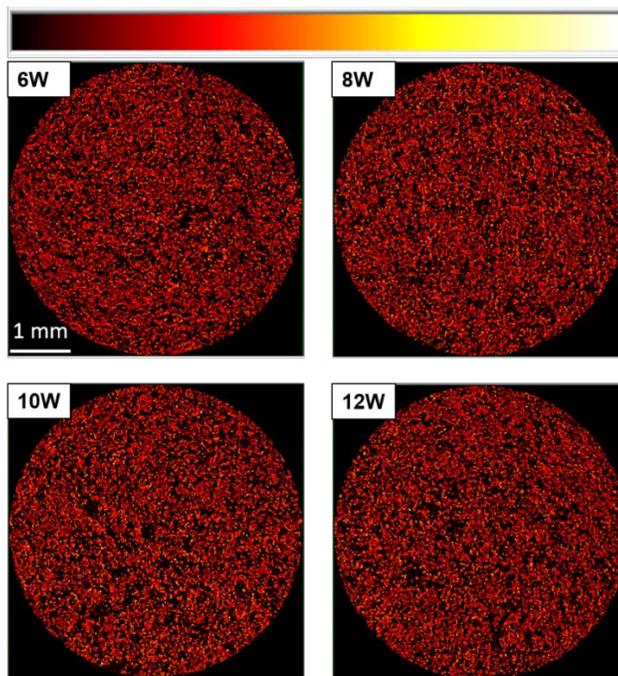

Figure 7: 2D images of cross section of UHMWPE parts produced
at vers

Figure 7 shows the cross-section images of the sintered parts at different laser powers. The dominated colour mainly ranges between red and orange, which indicates a low and medium density. High volume of pores can be observed at all levels of laser power (pores are in black colour). However, there is a fair amount of yellow dots can be seen within the structure as an indication of high density elements.

Morphological properties of the 3D structure of the UHMWPE LS parts, such as porosity, average pore diameter and pore size distribution were measured using micro-CT. In this study, two specimens were scanned for each laser power and the average results were obtained. The effect of laser power on porosity of the sintered parts measured by helium gas pycnometer and micro-CT is shown in Table 1.

Table 1: Porosity measurement of UHMWPE LS parts

Laser Power (watts)	Helium Pycnometer			Micro-CT		
	Total porosity (%)	Open pores (%)	Closed pores (%)	Total porosity (%)	Open pores (%)	Closed pores (%)
6	64.85	64.42	0.43	61.44	61.43	0.01
8	61.41	60.98	0.43	60.30	60.29	0.01
10	60.72	60.30	0.42	60.67	60.66	0.01
12	62.79	62.36	0.43	61.84	61.83	0.01

Figures 8, 9 and 10 show the average effect of laser power upon the total, open and closed porosities.
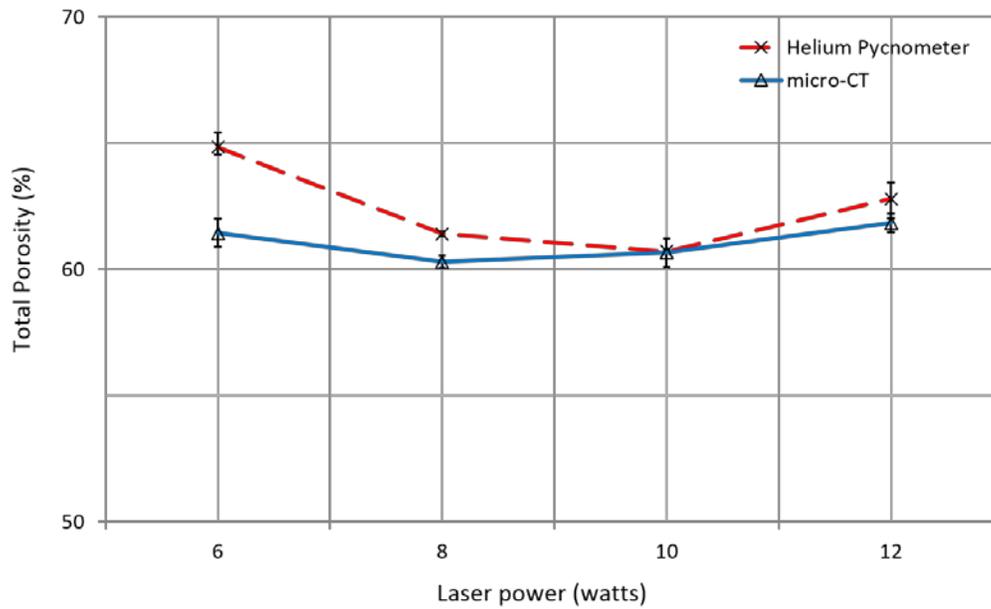
Figure 8: Average effect of laser power upon the porosity of the UHMWPE parts

A slight decrease of these porosities can be observed when the laser power increased from 6 to 10 watts. However, further increase in laser power (i.e. 12 watts) showed a slight increase in porosity. Gill et al [16] reported that polyamide LS parts built at higher energy density showed a reduction in porosity when compared to LS parts built at lower energy density. With increasing energy density from the optimum, the porosity increases due to degradation of the polymer.
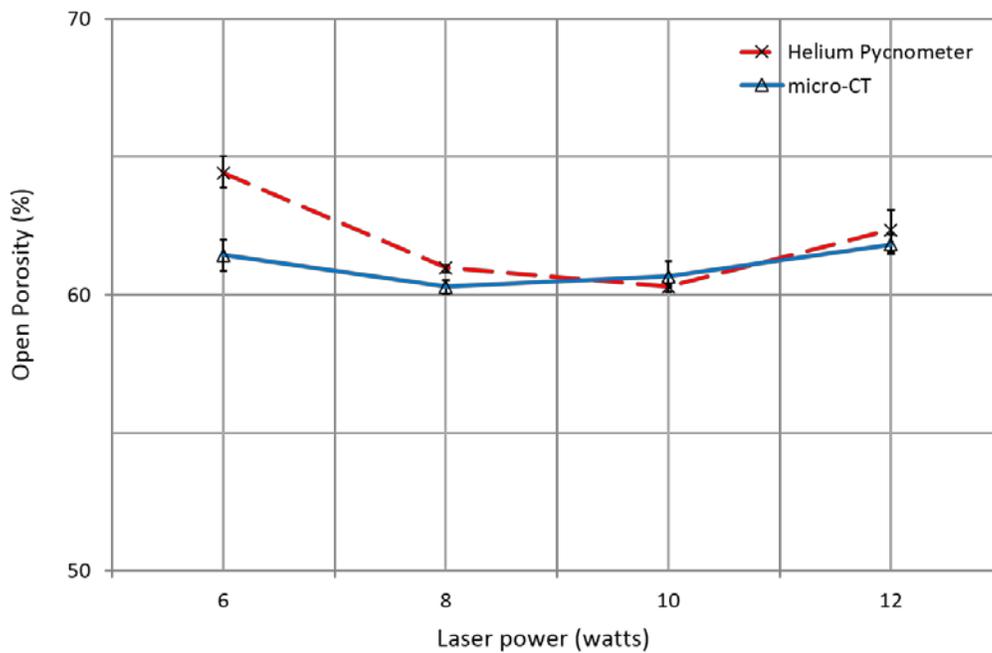
Figure 9: Average open porosity in UHMWPE parts produced at different laser powers

The change in the trend of total and open porosities measured by micro-CT technique is similar to the porosities measured using helium gas pycnometer method. There are no significant differences in the results obtained from both techniques and it is clear that the results fit very well with each other demonstrating the reliability of micro CT analysis.
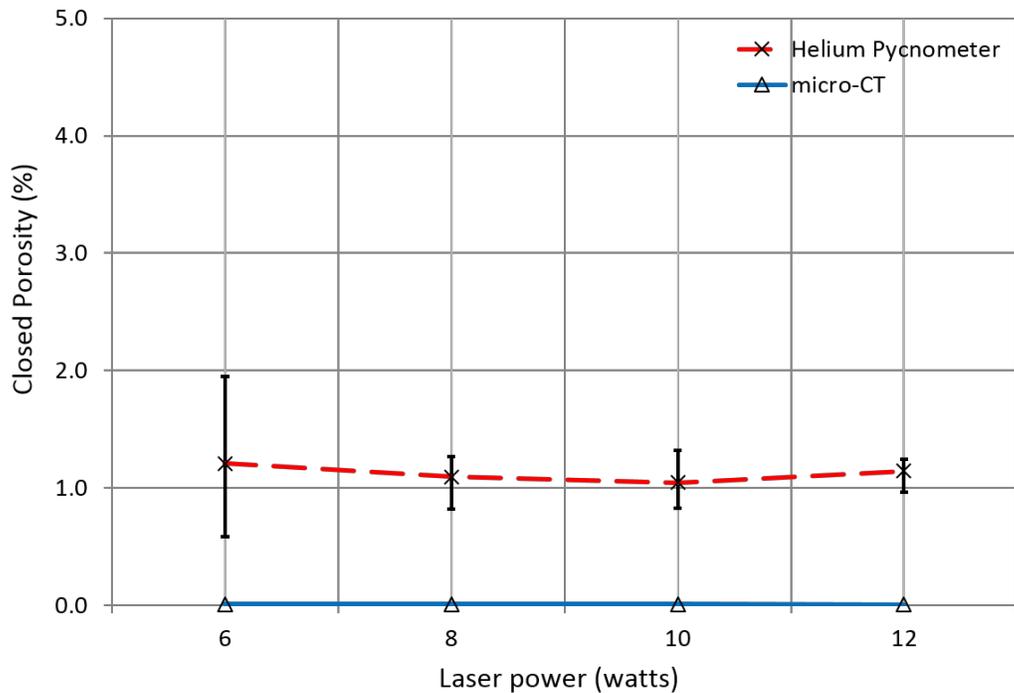
Figure 10: Average closed porosity in UHMWPE parts produced
at different laser powers

The closed porosity (Figure 10) remains fairly constant with increasing laser power. However, this result does not fit well with the result of the closed porosity obtained by micro-CT technique. This is very likely due to the fact that the volume of the closed porosity is low. Additionally, if the closed pores are in the same range as the scanning resolution of the micro-CT images, they may not be detected.

Figure 11 shows the effect of laser power on the average pore diameter. UHMWPE structure has a slightly larger pores at a laser power of 6 watts and the average pore diameter remains fairly constant with increasing laser power (i.e. 8, 10 and 12 watts).
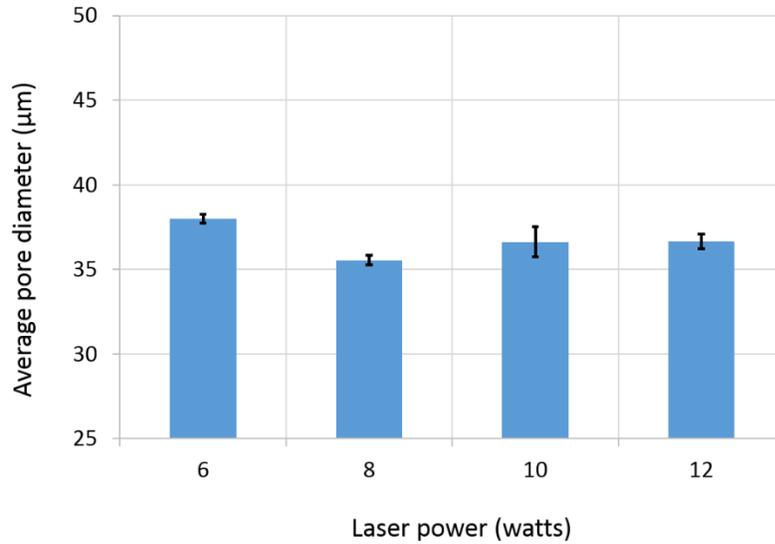
Figure 11: Average pore diameter of UHMWPE parts
produced at different laser powers

The cross-section (5 mm diameter) of the 2D micro-CT images in Figure 12 shows a similar characteristics at all levels of laser power.
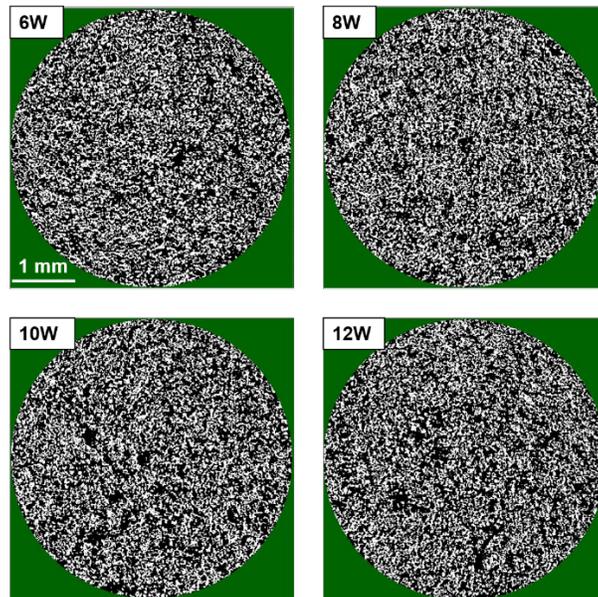

Figure 12: Cross-section of micro-CT binarised images of UHMWPE parts
produced at different laser powers (Pores in black colour)

Figure 13 shows the pore diameter distributions of LS parts at different laser powers. The volume of the pores with diameters in range between 30 – 40 µm is the highest for all levels of

laser power. Pore diameters larger than 40 and smaller than 89 are also present at all laser power levels and pore diameter larger than 89 µm can be seen clearly at laser power of 6 watts. However, the result shows that there is no statistically significant difference in the pore size distribution when the laser power is changed.
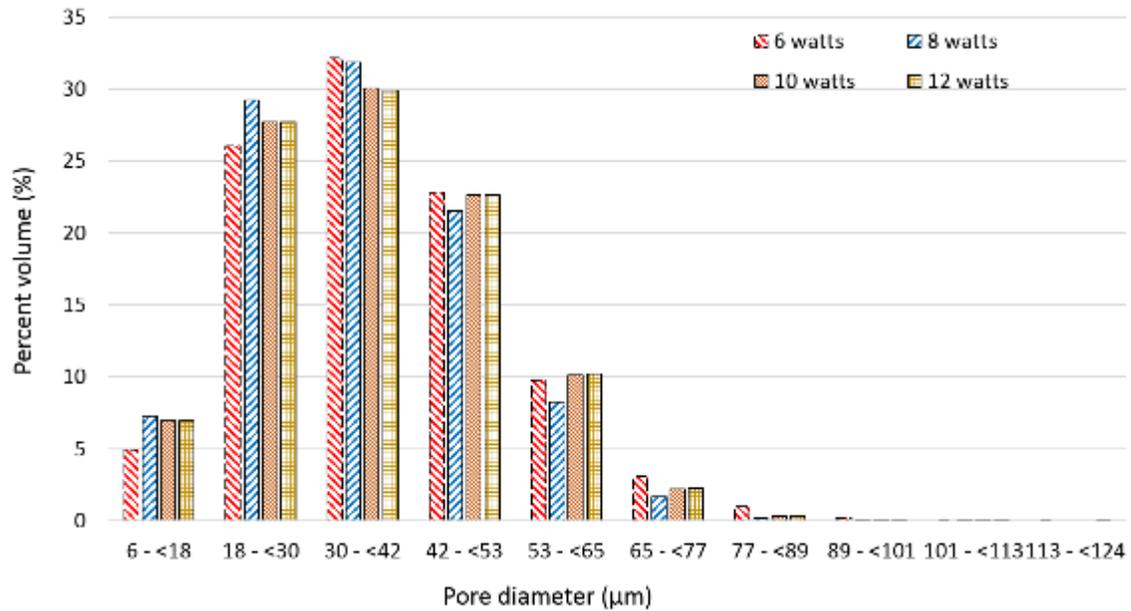

Figure 13: Pore size distribution of UHMWPE parts produced at different laser powers

4.2. Mechanical properties

Flexural stress-strain curves obtained by three point bend test analysis are shown in Figure 14.
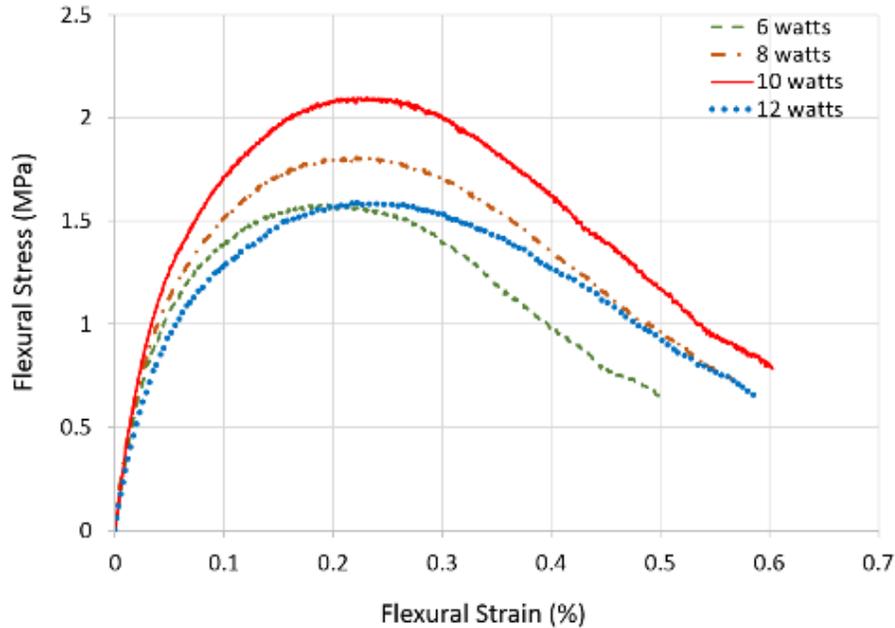

Figure 14: Flexural stress-strain curve of UHMWPE parts produced
at different laser powers

The result shows a less ductile behaviour for parts built at low laser powers than the parts built at higher laser power. The bonds between the powder particles, which occur due to the formation of more necking, become stronger at higher laser powers, which leads to a more ductile behaviour with a large plastic region in the stress–strain curve. This behaviour has been observed with Laser Sintering of other polymers [17]. However, at higher laser power, 12 watts, showed a decrease in maximum flexural stress and strain. Gill et al [16] observed this phenomena and reported that with increasing energy density from the optimum, degradation of the polymer occurs, which results in a reduction in strength.

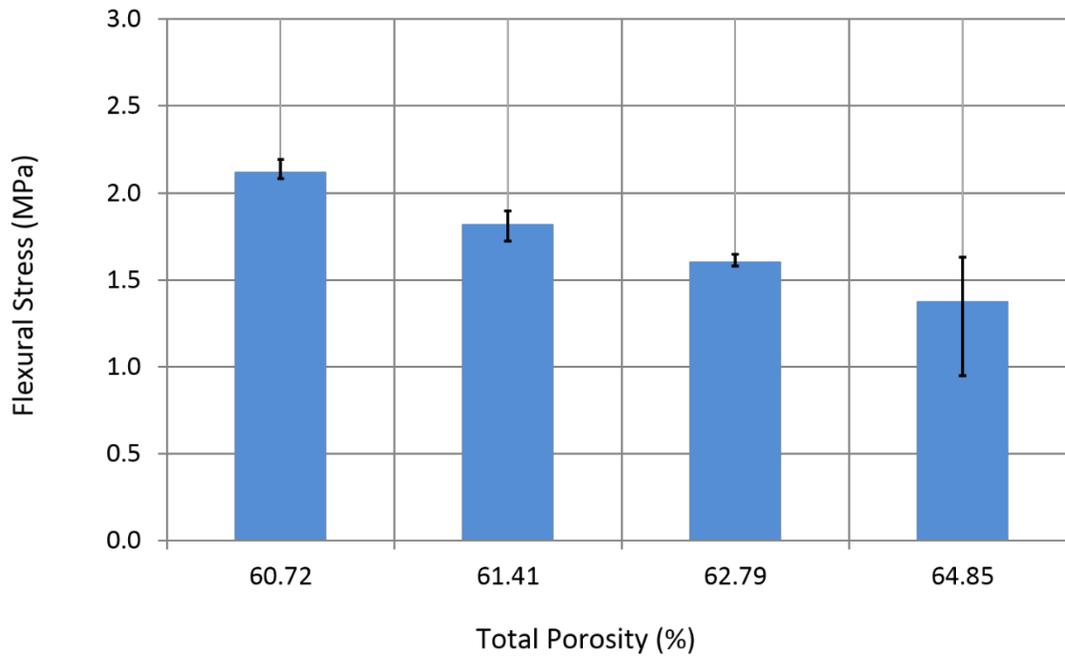Figure 15 shows the result of the flexural stress which was plotted versus the porosity of the LS parts.

Figure 15: Flexural stress vs total porosity of UHMWPE LS parts

The porosity results, obtained by the helium gas pycnometer method, show a typical change trend whereby the strength decreases as porosity increases. This behaviour was observed by Gill et al [16] and reported that the strength of LS parts decreases when the laser energy is insufficient to fully sinter the polymer, resulting in an increase in porosity.

4.3. Microstructure observation

Figures 16 and 17 show representative SEM images of the surface of the UHMWPE sintered parts at laser power of 6 and 8 watts respectively.
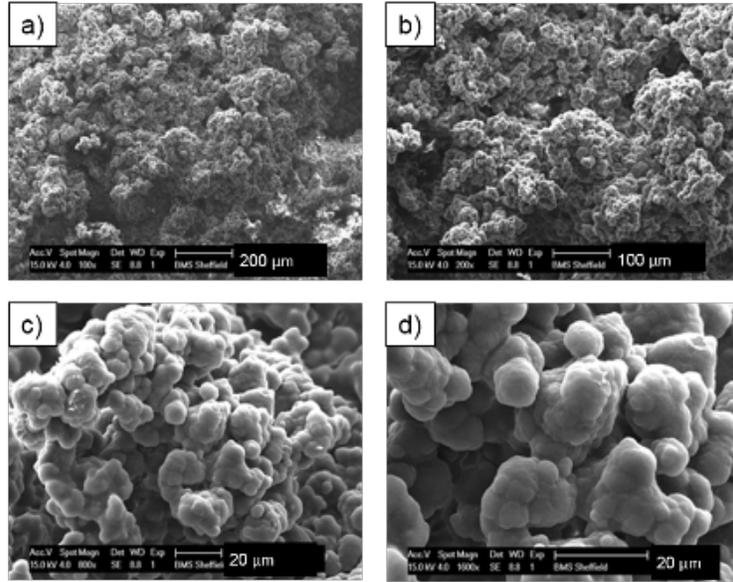
Figure 16: SEM micrographs of the sintered part of UHMWPE at laser power
of 6 watts with magnifications: a) 100x, b) 200x, c) 800x and (d) 1600x
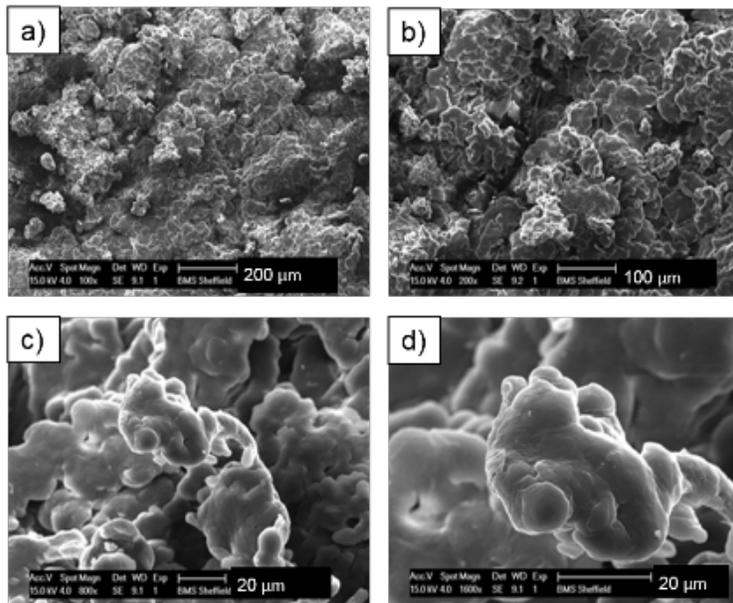

Figure 17: SEM micrographs of the sintered part of UHMWPE at laser power
of 8 watts with magnifications: a) 100x, b) 200x, c) 800x and (d) 1600x

The porous structure can be seen in both samples but with different forms. The SEM observation showed that when the laser power increased from 6 to 8 watts, the UHMWPE LS parts became denser with a higher degree of coalescence. It seems that the fusion of the polymer particles

becomes better with a more compact morphology when the laser power increases to a certain levels [18].

5. Conclusions

The following conclusions are made from this study:

- The results showed a high level of porosity in the UHMWPE LS parts with a range of 60-65% measured by micro-CT and helium gas pycnometer method respectively. A slight decrease in porosity was observed when the laser power increased from 6 to 10 watts. Further increase in laser power to 12 watts showed a slight increase in porosity.

- The change in the trend of total and open porosities measured by micro-CT technique is similar to the porosities measured using helium gas pycnometer. There are no significant differences in the results obtained from both techniques. The results fit very well with each other demonstrating the suitability and reliability of micro CT for morphology characterisation.

- The UHMWPE samples have slightly larger pores at a laser power of 6 watts and the average pore diameter remains fairly constant with the increase in laser power (i.e. 8, 10 and 12 watts).

- The flexural stress-strain result revealed a less ductile behaviour for parts built at low laser powers than the parts built at higher laser power. However, at higher laser power (i.e. 12 watts) a decrease in maximum flexural stress and strain was observed.

- The porosity results, obtained by helium gas pycnometer, combined with the flexural measurements, showed that the flexural strength decreases as the porosity increases.

References

1.   Kerckhofs, G., Pyka, G., Loeckx, D., Van Bael, S., Schrooten, J., and Wevers, M. *The combined use of micro-CT imaging, in-situ loading and non-rigid image registration for 3D experimental local strain mapping on porous bone tissue engineering scaffolds under compressive loading*.

2.   De Chiffre, L., Carmignato, S., Kruth, J.P., Schmitt, R., and Weckenmann, A., *Industrial applications of computed tomography*. CIRP Annals - Manufacturing Technology, 2014. **63**(2): p. 655-677.

3.   Bourell, D.L., Watt, T.J., Leigh, D.K., and Fulcher, B., *Performance Limitations in Polymer Laser Sintering*. Physics Procedia, 2014. **56**(0): p. 147-156.

4.   Goodridge, R.D., Hague, R.J.M., and Tuck, C.J., *An empirical study into laser sintering of ultra-high molecular weight polyethylene (UHMWPE)*. Journal of Materials Processing Technology, 2010. **210**(1): p. 72-80.

5.   Pyka, G., Van de Casteele, E., Depypere, M., Kerckhofs, G., Schrooten, J., Maes, F., and Wevers, M. *Evaluation of credibility and limitations of the non-rigid registration of micro-CT images as a tool for local strain analysis*. in *Micro-CT User Meeting*. 2014.

6.   Pradhan, S.K., Dwarakadasa, E.S., and Reucroft, P.J., *Processing and characterization of coconut shell powder filled UHMWPE*. Materials Science and Engineering: A, 2004. **367**(1–2): p. 57-62.

7.   Deplancke, T., Lame, O., Rousset, F., Aguili, I., Seguela, R., and Vigier, G., *Diffusion versus Cocrystallization of Very Long Polymer Chains at Interfaces: Experimental Study of Sintering of UHMWPE Nascent Powder*. Macromolecules, 2014. **47**(1): p. 197-207.

8.   Turell, M.B. and Bellare, A., *A study of the nanostructure and tensile properties of ultra-high molecular weight polyethylene*. Biomaterials, 2004. **25**(17): p. 3389-3398.

9.   Kelly, A., *Concise Encyclopedia of Composite Materials*. 2012: Elsevier Science.

10.   Rimell, J.T. and Marquis, P.M., *Selective laser sintering of ultra high molecular weight polyethylene for clinical applications*. Journal of Biomedical Materials Research, 2000. **53**(4): p. 414-420.

11.   Dupin, S., Lame, O., Barrès, C., and Charmeau, J.-Y., *Microstructural origin of physical and mechanical properties of polyamide 12 processed by laser sintering*. European Polymer Journal, 2012. **48**(9): p. 1611-1621.

12.   Rouholamin, D. and Hopkinson, N., *An investigation on the suitability of micro-computed tomography as a non-destructive technique to assess the morphology of laser sintered nylon 12 parts*. Proceedings of the Institution of Mechanical Engineers, Part B: Journal of Engineering Manufacture, 2014. **228**(12): p. 1529-1542.

13. Ho, S.T. and Hutmacher, D.W., *A comparison of micro CT with other techniques used in the characterization of scaffolds.* Biomaterials, 2006. **27**(8): p. 1362-1376.

14. Rüsenberg, S., Schmidt, L., and Schmid, H. *Mechanical and physical properties–a way to assess quality of laser sintered parts.* in *Proceedings of the 22nd International Solid Freeform Fabrication Symposium*. 2011.

15. Ajoku, U., Saleh, N., Hopkinson, N., Hague, R., and Erasenthiran, P., *Investigating mechanical anisotropy and end-of-vector effect in laser-sintered nylon parts.* Proceedings of the Institution of Mechanical Engineers, Part B: Journal of Engineering Manufacture, 2006. **220**(7): p. 1077-1086.

16. Gill, T.J. and Hon, K.K.B., *Experimental investigation into the selective laser sintering of silicon carbide polyamide composites.* Proceedings of the Institution of Mechanical Engineers, Part B: Journal of Engineering Manufacture, 2004. **218**(10): p. 1249-1256.

17. Caulfield, B., McHugh, P.E., and Lohfeld, S., *Dependence of mechanical properties of polyamide components on build parameters in the SLS process.* Journal of Materials Processing Technology, 2007. **182**(1–3): p. 477-488.

18. Ho, H.C.H., Gibson, I., and Cheung, W.L., *Effects of energy density on morphology and properties of selective laser sintered polycarbonate.* Journal of Materials Processing Technology, 1999. **89–90**: p. 204-210.